Electronic Supplementary Material (ESI) for Physical Chemistry Chemical Physics.
This journal is © the Owner Societies 2022

# Superior mechanical flexibility, lattice thermal conductivity and electron mobility of the hexagonal honeycomb carbon nitride monolayer

Tian Zhang [†*], Jia-He Lin[§], and Xiao Jia[†,‡*]

†*School of Physics and Electronic Engineering, Sichuan Normal University, Chengdu 610066, China*

‡ *School of Mathematical Science, University of Electronic Science and Technology of China, Chengdu 610054, China*

§*School of Science, Jimei University, Xiamen 361021, China*

[*]*e-mail:zhangt512@foxmail.com;xiaojia@sicnu.edu.cn*

**ABSTRACT: Nitrogen is the nearest neighbor element of carbon, and thus the hexagonal honeycomb carbon nitride monolayer ($C_xN_y$) consisted of a covalent network of carbon and nitrogen atoms can usually own attractive physical and chemical properties similar to those in graphene. Here, we systematically investigate the geometric structure, mechanical properties, thermal transport properties, and plasmon excitation of a new phase labeled $C_3N_2$, and make a detailed comparison with other possible $C_xN_y$ allotropes. All $C_xN_y$ own the super-high layer modulus and Young's modulus. But compared with others, the $C_3N_2$ exhibits its excellent mechanical flexibility, which can withstand relatively high critical strain up to 20% (18%) along X (Y) direction. Additionally, the $C_3N_2$ also own the excellent thermal and electronic transport properties with the super-high lattice thermal conductivity ~ 110.9 W/mK**

**and electron mobility ~ 1617.52 $cm^2/V{\cdot}s$ at 300 K. By performing the time-dependent density functional theory (TDDFT), we obtain optical absorptions of the $C_3N_2$ and $C_3N$, and meanwhile analyze their Fourier transforms of induced charge densities at some resonant frequencies. The main optical absorption peaks of the $C_3N_2$ nanostructure are located in ultraviolet region, and its plasmon peaks are far higher than those in the $C_3N$. Excellent mechanical and optical properties, the larger electronic band gap, and the higher electron mobility promote the $C_3N_2$ with great potential for application in nanoelectronics and optoelectronics.**

**Keywords: Carbon nitride monolayers; Mechanical properties; Lattice thermal conductivity; Electron mobility; Plasmon excitation; Time-dependent density functional theory (TDDFT);**

Table S1: Calculated effective masses $m^*$ ($m_0$), average effective masses $m_d$ ($m_0$), elastic modulus $C_{2D}$ (eV/Å$^2$), deformation energies $E_l$ (eV), carrier mobilities $\mu$ (cm$^2$/Vs) and relaxation time $\tau$ ($10^{-14}$ s) for the $C_3N_2$ and $C_3N$ at 300 K by performing PBE-GGA method.

| | $E_l$ (eV) | $C_{2D}$ (eV/Å$^2$) | $m^*$ ($m_0$) | $m_d$ ($m_0$) | $\mu$ (cm$^2$/V $\cdot$ s) | $\tau$ ($10^{-14}$ s) |
|---|---|---|---|---|---|---|
| $C_3N_2$ | | | | | | |
| Hole | 3.05 | 16.44 | 3.79 | 3.15 | 50.86 | 8.97 |
| Electron | 3.40 | 16.44 | 0.52 | 0.58 | 1617.52 | 52.63 |
| $C_3N$ | | | | | | |
| Hole | 5.35 | 26.69 | 0.55 | 0.74 | 785.74 | 32.62 |
| Electron | 5.24 | 26.69 | 0.72 | 0.77 | 605.24 | 25.97 |

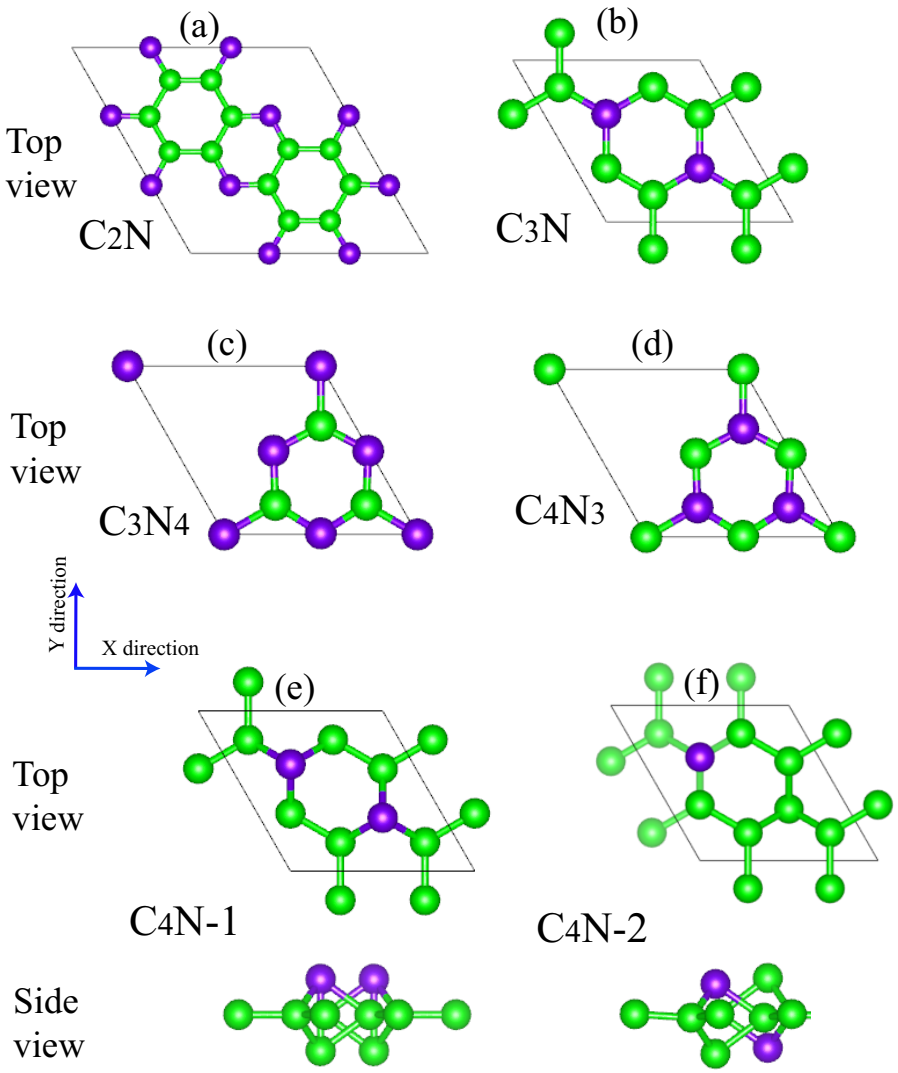


**Figure S1.** Top and side views of the (a) the $C_2N$, (b) $C_3N$, (c) $C_3N_4$, (d) $C_4N_3$, (e) $C_4N$-1, and (f) $C_4N$-1 structure.

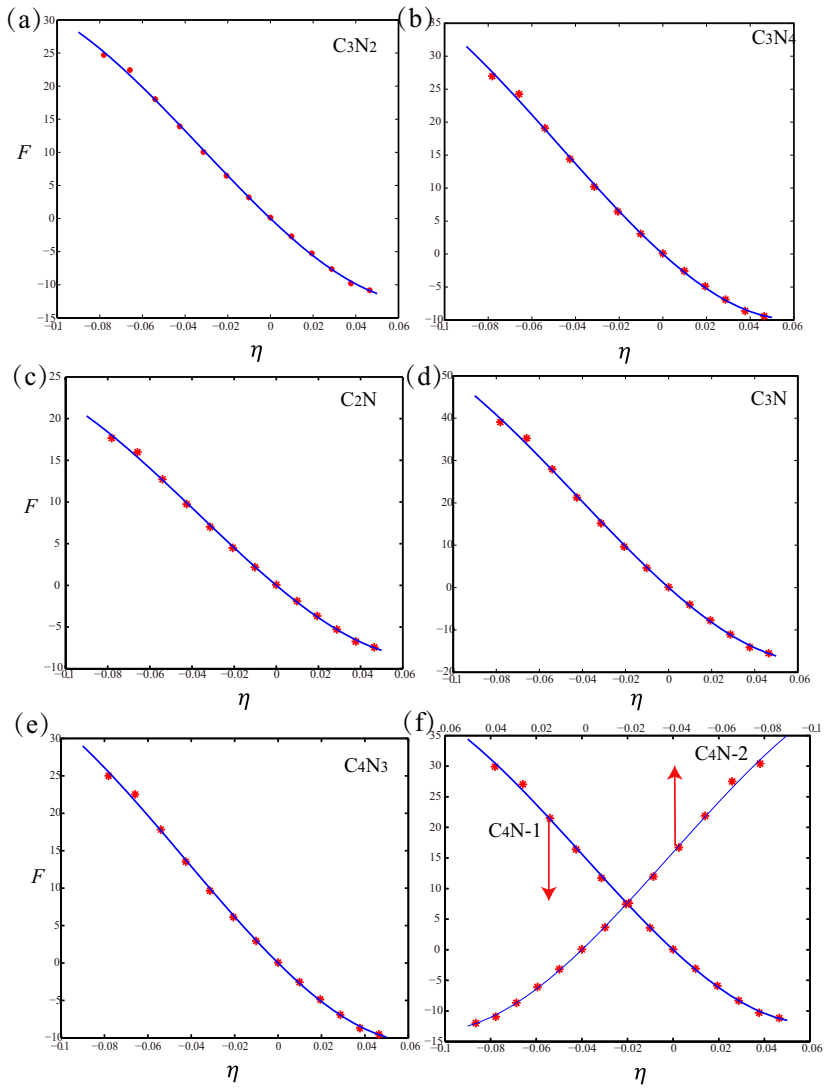


**Figure S2.** The calculated forces per unit length ($F$) of the (a) $C_3N_2$, (b) $C_3N_4$, (c) $C_2N$, (d) $C_3N$, (e) $C_4N_3$, and (f) $C_4N$-1 and $C_4N$-1 as a function of the $\eta$.

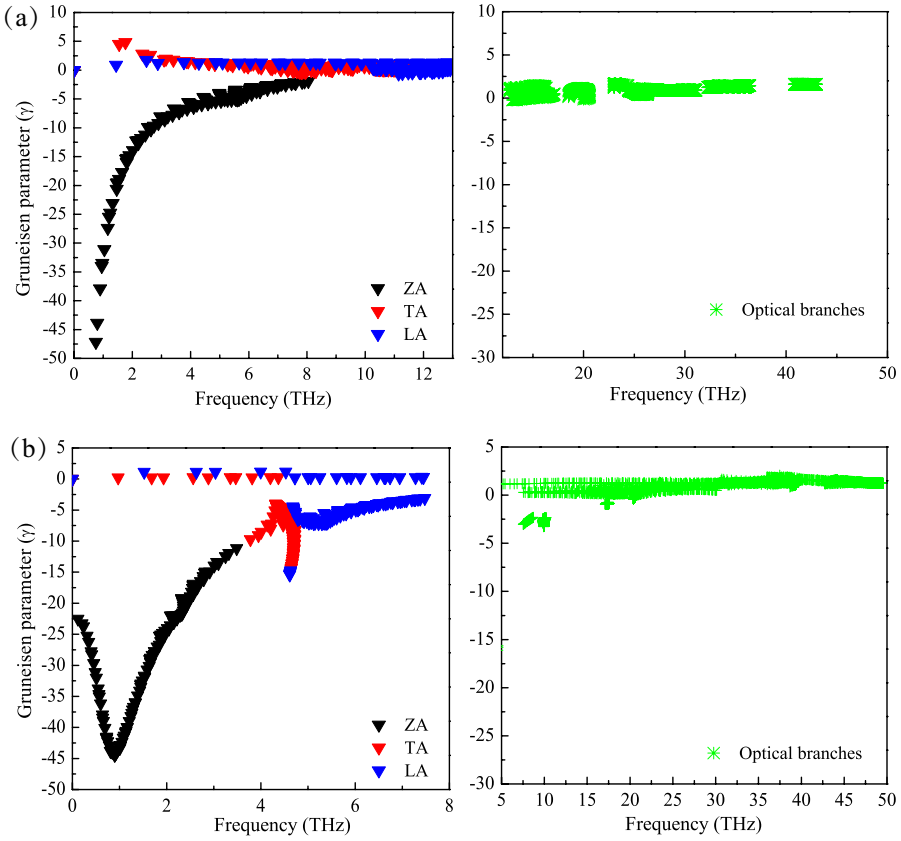


**Figure S3.** The Grüneisen parameters $\gamma$ of the (a) $C_3N_2$ and (b) $C_3N$ for all phonon branches.

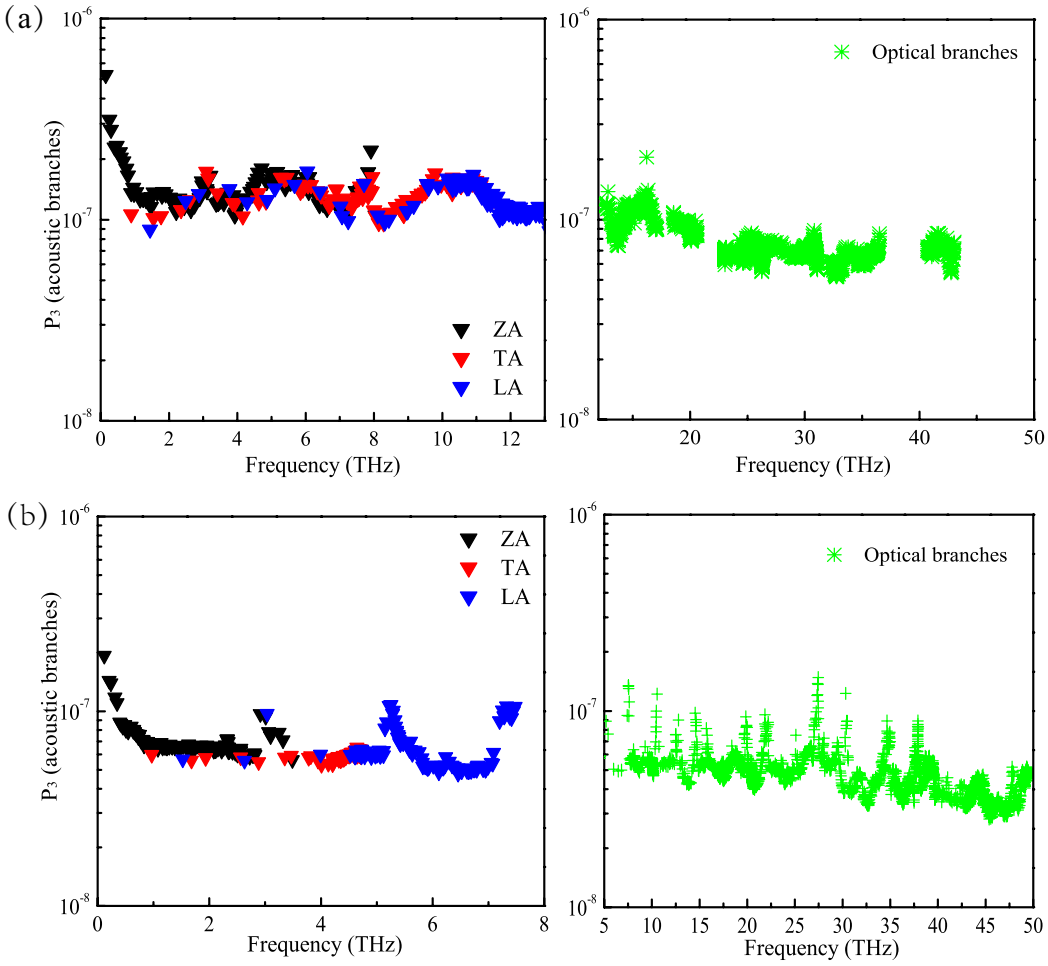


**Figure S4.** The calculated phase space *P*3 of the (a) $C_3N_2$ and (b) $C_3N$ for all phonon branches.

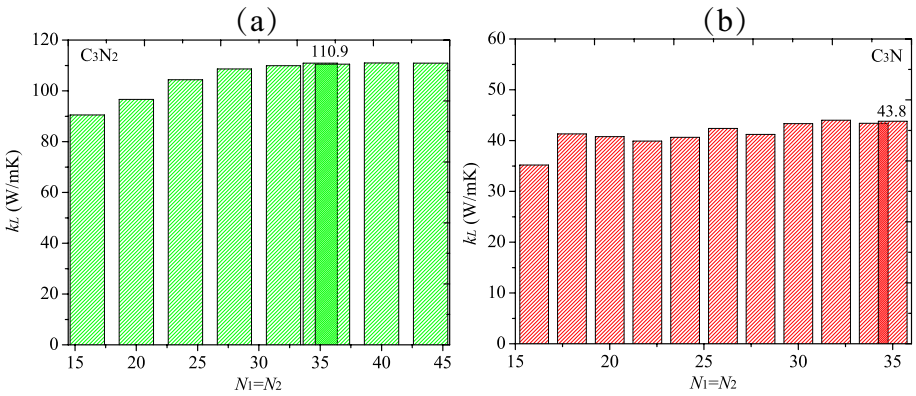


**Figure S5.** The calculated lattice thermal conductivities $k_L$ of the (a) $C_3N_2$ and (b) $C_3N$ for different numbers of $q$ points along $\vec{a}_1$ and $\vec{a}_2$ directions at 300 K.

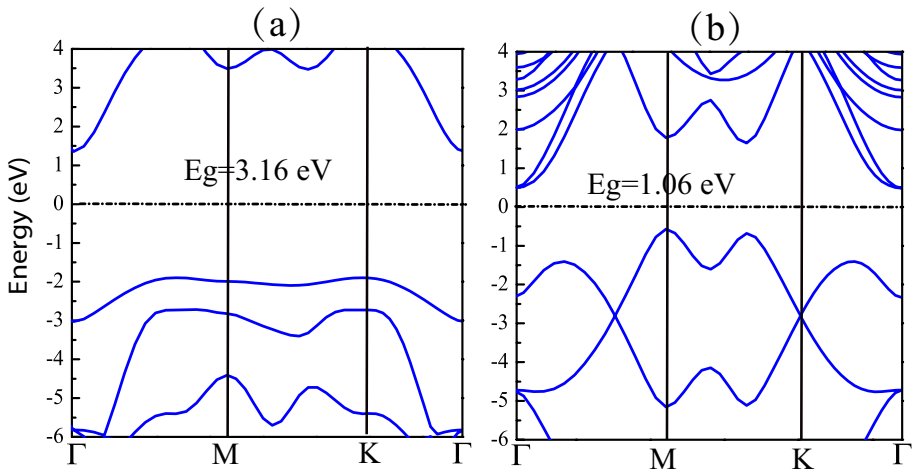


**Figure S6.** The calculated electronic band structures of the (a) $C_3N_2$ and (b) $C_3N$ based on HSE06 method.

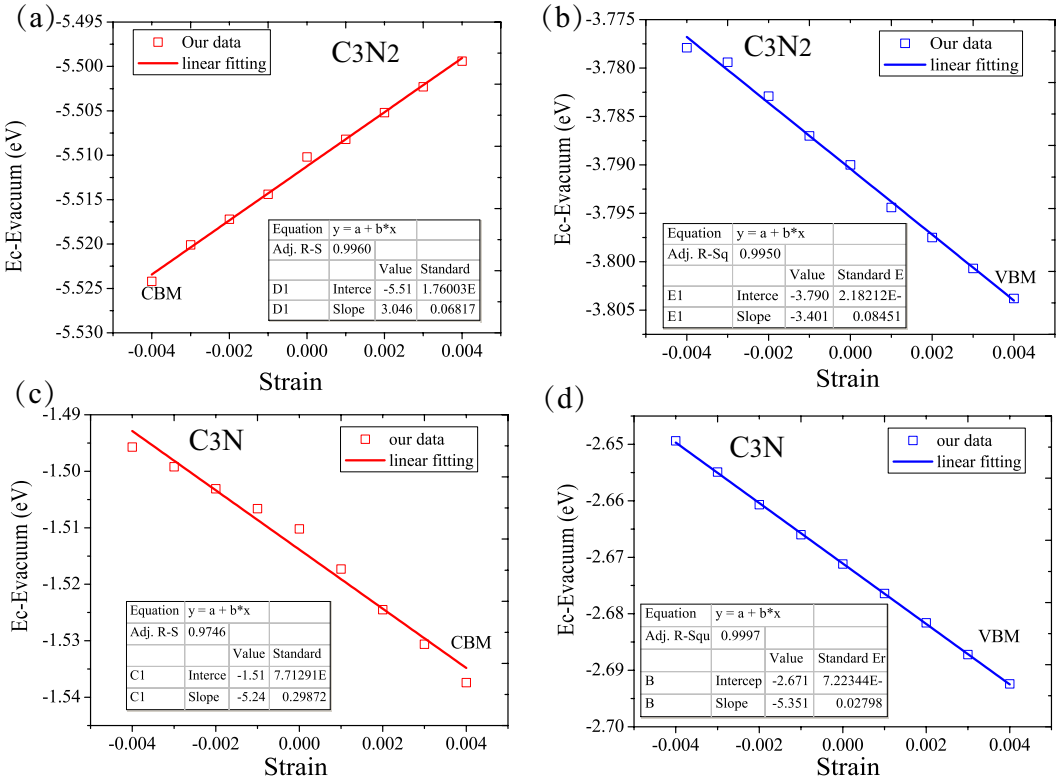


**Figure S7.** The band edges versus uniaxial strain for the $C_3N_2$ [(a) and (b)] and $C_3N$ [(c) and (d)] based on PBE-GGA method.

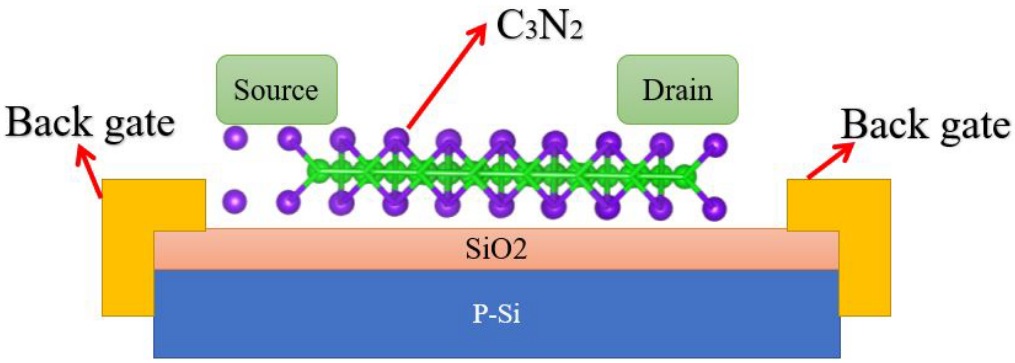


**Figure S8.** The schematic of $C_3N_2$-based field effect transistors (FET) device, with the drain, source, and back-gate electrodes.